



Research Article

***Calotropis gigantea* Assisted Synthesis of Zinc Oxide Nanoparticle Catalysis: Synthesis of Novel 3-Amino Thymoquinone Connected 1,4-Dihydropyridine Derivatives and Their Cytotoxic Activity**

Perumal Gobinath,¹ Ponnusamy Packialakshmi,¹ Ashraf Atef Hatamleh,² Munirah Abdullah Al-Dosary,² Yasmeen Abdualrhman Al-Wasel,² Ravindran Balasubramani,³ Radhakrishnan Surendrakumar ¹, and Akbar Idhayadhulla ¹

¹PG & Research, Department of Chemistry, Nehru Memorial College (Affiliated Bharathidasan University), Puthanampatti, South India, Tamil Nadu, India

²Department of Botany and Microbiology, College of Science, King Saud University, P.O. Box 2455, Riyadh 11451, Saudi Arabia

³Department of Environmental Energy and Engineering, Kyonggi University, Suwon 16227, Republic of Korea

Correspondence should be addressed to Radhakrishnan Surendrakumar; surendrakumar@nmc.ac.in and Akbar Idhayadhulla; a.idhayadhulla@gmail.com

Received 21 May 2021; Accepted 29 March 2022; Published 23 April 2022

Academic Editor: P. Davide Cozzoli

Copyright © 2022 Perumal Gobinath et al. This is an open access article distributed under the Creative Commons Attribution License, which permits unrestricted use, distribution, and reproduction in any medium, provided the original work is properly cited.

The synthesis of biologically active 1,4-dihydropyridine derivatives using a *Calotropis gigantea* leaf powder and ZnO NPs used as catalyst under solvent-free conditions at room temperature via grinding method has been established in a single-stage, mild, and environmentally friendly green process. The procedure is fast and effective and produces high yields. Three cancer cell lines were used to assess the cytotoxic activity of 1,4-dihydropyridine derivatives. The cytotoxicity of 1,4-dihydropyridine compound **1f** (HepG2, LC₅₀-0.50 μM, MCF-7, LC₅₀-0.64 μM, and HeLa, LC₅₀-0.52 μM) was found to be highly active. The synthesized derivatives demonstrated their safety by causing substantially less cytotoxicity in normal cell lines HEK-293, LO2, and MRC5 with IC₅₀ > 100 g/mL. As a result, compound **1f** could serve as a high-impact molecule for the production of anticancer drugs in the future.

1. Introduction

Green synthesis of nanoparticles has received a lot of attention in recent years as a simple, inexpensive, and environmentally friendly alternative to chemical and physical synthesis methods. Cancer is a term used to describe a group of more than 100 diseases that include the irregular and uncontrolled division of cells and affect major body organs [1, 2]. Cancer has surpassed tobacco as the second leading cause of death worldwide, accounting for 1 in every 6 deaths

in 2018, with a total of 9.6 million deaths. Different forms of cancers have affected both men and women [3]. Resistance to current multidrug chemotherapy is their slow cure rate, as well as their dreadful and toxic side effects on patients [4]. As a result, exemplary efforts are needed to identify newer, more efficient, and less toxic chemotherapeutic agents for the treatment of cancers [5].

TQ has antioxidant, anti-inflammatory, and cancer-fighting chemical structures which are shown in Figure 1. TQ has been shown to be effective in the treatment of

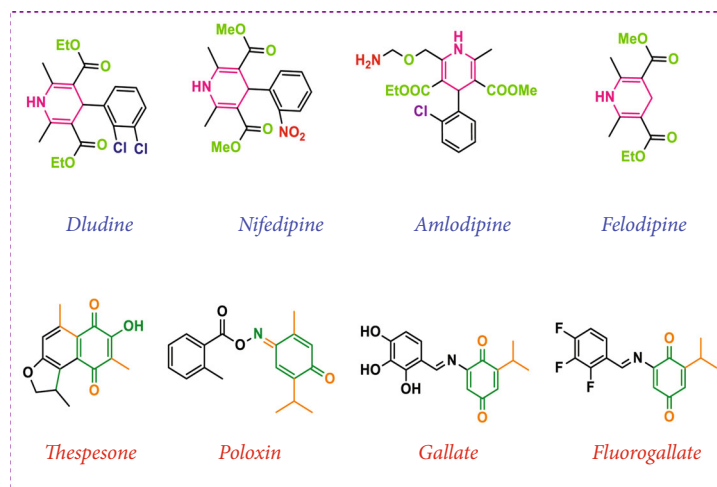


FIGURE 1: Biologically active compounds of thymoquinone and 1,4-dihydropyridine derivatives.

symptoms in a variety of disease models, including cancer, diabetes, asthma, encephalomyelitis, and arthritis [6]. Thymoquinone serves as a potent antioxidant in normal tissues, inhibiting superoxide radical synthesis and lipid peroxidation while also increasing the activities of antioxidant enzymes such as SOD, catalase, GSH, GST, and quinone reductase [7].

TQ is a naturally occurring phytochemical compound that is the main constituent of *Nigella sativa* (black seed) volatile oil and was first isolated in 1963 by El-Dakhakhny [8]. Both *in vitro* and *in vivo*, this monoterpene was found to have potent anticancer properties [9–11]. TQ induces apoptosis *in vitro* through p53-dependent and p53-independent pathways, while causing no toxicity in normal cells, according to recent research [12, 13]. TQ, as a short-chain ubiquinone derivative, can act as a prooxidant and thus cause oxidative stress by triggering the development of reactive oxygen species (ROS) [14], which has been related to its proapoptotic effect in colon cancer and leukaemia cells [15, 16]. TQ has recently been shown to suppress metastasis in CPT-11-R LoVo colon cancer cells by inhibiting NF- κ B and activating JNK and p38, as well as to prevent epithelial–mesenchymal transformation in cancer cells by inhibiting the PI3K/AKT signalling axis [17, 18]. In addition, *in vivo* tests revealed that TQ has a low overall toxicity [19, 20], making it a viable candidate for clinical applications [21]. TQ has been shown to improve the effectiveness of many chemotherapeutic agents *in vitro* and *in vivo*, including in cancers that are immune to them, such as cisplatin in lung cancer and many solid tumours [22, 23]. Many researchers have written on the possible utility of ZnO nanoparticles in the treatment of cancer in recent years in the biological field. It has been investigated as an effective catalyst for several organic transformations [17–21], such as the Mannich reaction and the Knoevenagel condensation reaction, in the synthesis of coumarin, due to various advantages associated with its eco-friendly nature.

Calcium channel blockers, cardiovascular, antihypertensive, antitumor, anti-inflammatory, analgesic, neuroprotectant, platelet antiaggregator, anti-ischemic, anti-Alzheimer,

antimicrobial, and insecticidal are some of the biological functions of 1,4-DHP structures which are shown in Figure 1 [24–30].

Aside from their biological significance, 1,4-DHPs are useful sources of hydride for reductive amination and synthetic intermediates for the production of biologically significant molecules [31]. Since Hantzsch's first classical study on the synthesis of 1,4-DHPs by multicomponent reactions (MCR) in 1882 [32], there has been a lot of interest in improving and developing new methods to generate therapeutically relevant molecules [33]. MCR has been focusing on the development of highly diverse and functionalized molecules in recent years [34–43]. In certain cases, these synthetic hybrids with partial natural compound structures are more active than their parent compounds [44, 45]. To our knowledge, no thymoquinone-linked 1,4-dihydropyridine derivatives have been identified using the grindstone method in the presence of ZnO NP catalyst. As a result, the natural product TQ can be considered a promising anticancer active compound that is ideal for using the Hantzsch method to create new potent anticancer agents.

2. Materials and Methods

2.1. General Methods. All the melting points were determined in open capillary tubes and are uncorrected. The FT-IR spectra were recorded the KBr disk technique on a Shimadzu 8201pc (4000–1000 cm^{-1}). The $^1\text{H-NMR}$ and $^{13}\text{C-NMR}$ spectra were recorded on a Bruker DRX-300 MHz. For SEM research, a Scanning Electron Microscope (SEM) model VP-1450 (LEO, Co., Germany) was used. An LEO 912 AB transmission electron microscopy (TEM) instrument was used for the study. Mass spectra were recorded by Perkin Elmer GCMS model Clarus SQ8 (EI). The elemental analysis (C, H, and N) was performed using an elemental analyser model (Varian EL III). TLC was used to verify the purity of each compound using silica-gel, 60F254 aluminium sheets as adsorbent, and iodine used for visualization.

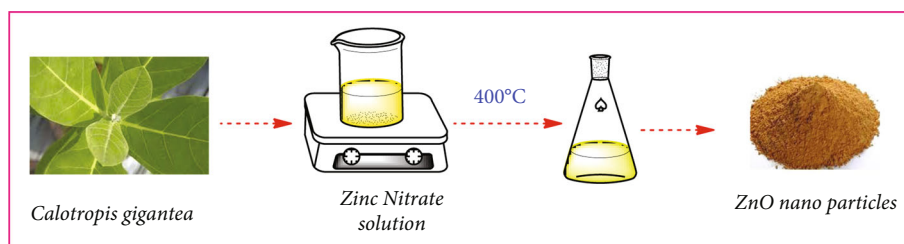
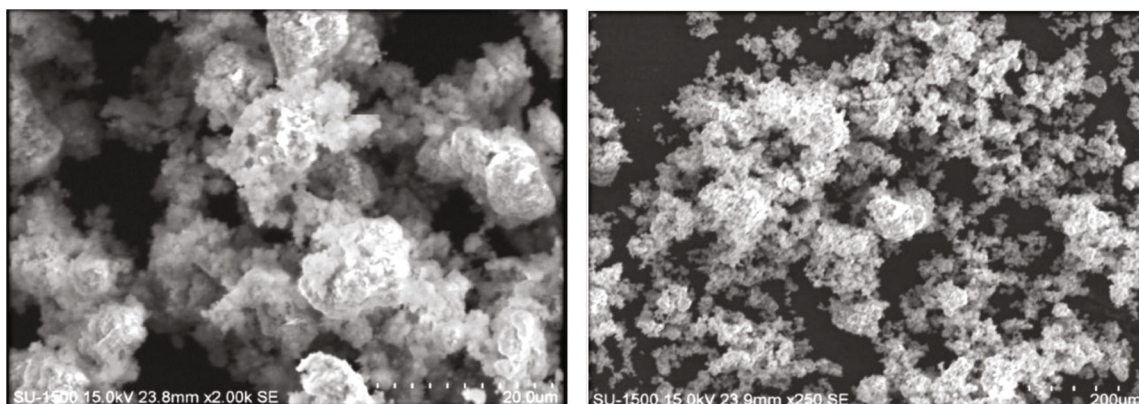
SCHEME 1: Synthesis of ZnO nanoparticles from *C. gigantea*.

FIGURE 2: SEM image of ZnO nanoparticle.

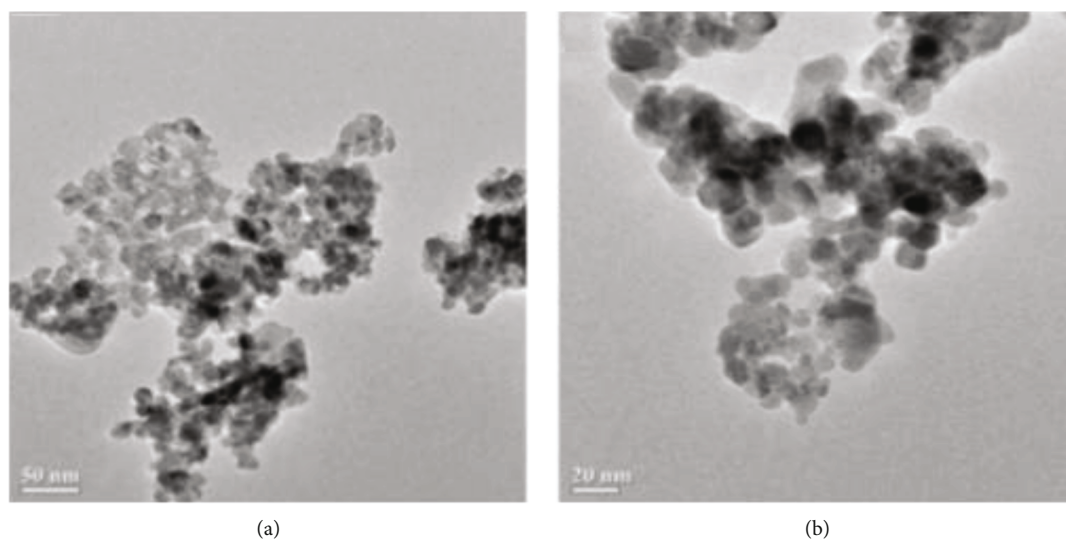


FIGURE 3: (a, b) TEM images of ZnO NPs with different magnifications.

2.1.1. Preparation of the *Calotropis gigantea* Leaf Extract. The extract for the reduction of zinc ions (Zn^{2+}) to zinc nanoparticles (ZnO) was made by combining 60 g of washed dried fine cut leaves with 200 mL of sterile distilled water in a 250 mL glass beaker. After that, the mixture was boiled for 60 minutes or until the aqueous solution's colour changed from watery to light yellow. The extract was allowed to cool to room temperature before being filtered onto filter paper. To be used in future research, the extract was kept in the refrigerator.

2.1.2. Preparation of Zinc Nanoparticles. A stirrer-heater was used to boil 60 mL of *C. gigantea* leaf extract to 70-80 degrees Celsius for the synthesis nanoparticle. As the temperature reached 70 degrees Celsius, 5 grammes of zinc nitrate was applied to the solution. This mixture is then reduced to a deep yellow paste by boiling it. This paste was then deposited in a ceramic crucible and heated for 3 hours at 350 degrees Celsius in an air-heated furnace. For characterization purposes, a light-yellow powder was obtained and carefully collected and packed. To obtain a finer nature

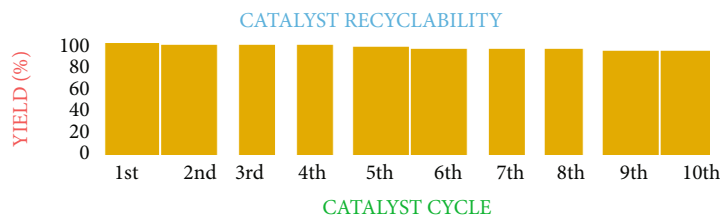


FIGURE 4: Recyclability of ZnO nanoparticle.

TABLE 1: Catalyst recyclability.

Entry	Catalyst use	Yield (%)
1	1 st	80
2	2 nd	90
3	3 rd	88
4	4 th	86
5	5 th	83
6	6 th	91
7	7 th	90
8	8 th	92
9	9 th	89
10	10 th	86

for characterization, the substance was mashed in a mortar-pestle. Scheme 1 depicts the synthesis of ZnO-NPs.

2.1.3. General Procedure for the Synthesis of Diethyl 1-(2-Isopropyl-5-methyl-3,6-dioxocyclohexa-1,4-dien-1-yl)-2,6-dimethyl-4-phenyl-1,4-dihydropyridine-3,5-dicarboxylate (1a). A reaction mixture consisting of ethyl acetoacetate (0.01 mol, 1.3 mL), benzaldehyde (0.01 mol, 1.06 mL), and 3-aminothymoquinone (0.01 mol, 1.80 g) with green catalyst ZnO NPs was mixed in a mortar and ground for up to 15-20 min at room temperature. Subsequently, the product was washed with excess ice-cold water, and then, the product was filtered and washed with water and dried to afford the crude product. The crude precipitate dissolved in DMF and centrifuged to separate the catalyst and later the catalyst was washed several times with EtOH, then dried, and reutilized three times for the same reaction. Then, the product was confirmed via TLC. The precipitate was recrystallized with ethanol. The product was obtained in excellent yield. The same method was followed for the synthesis of compounds **1b-j**.

(1) Synthesis of Diethyl 1-(2-Isopropyl-5-methyl-3,6-dioxocyclohexa-1,4-dien-1-yl)-2,6-dimethyl-4-phenyl-1,4-dihydropyridine-3,5-dicarboxylate (1a). The results are as follows: dark red solid, yield 85%; mp 46°C; IR (kBr) (cm⁻¹): 3028 (Ar-H), 2948, 2820 (C-H str of CH₃), 1745 (C=O in ester), 1650, 1620 (C=O); ¹H NMR (300 MHz, DMSO-d₆): 7.26-7.23 (m, 5H, Ph), 6.29 (s, 1H, -CH in TQ), 4.93 (s, 1H, CH-Ph), 4.16 (m, 4H, -(CH₂)₂), 2.52 (m, 1H, CH in TQ),

2.26 (s, 6H, 2,6-CH₃), 1.73 (s, 3H, -CH₃), 1.22 (t, 6H, -(CH₃)₂), 1.06 (d, *J* = 6.7 Hz, CH₃); ¹³C NMR (300 MHz, DMSO-d₆): 187.21, 178.53, 167.25, 153.57, 144.69, 144.41, 143.82, 142.73, 133.84, 128.65, 127.76, 125.77, 102.38, 61.79, 43.53, 21.02, 15.44, 14.26, 14.18; EI-MS: 491 (M⁺, 20%); elemental analysis (C₂₉H₃₃NO₆): calculated: C, 70.86; H, 6.77; N, 2.85%; found: C, 70.84; H, 6.75; N, 2.83%.

(2) Synthesis of Diethyl 4-(4-Chlorophenyl)-1-(2-isopropyl-5-methyl-3,6-dioxocyclohexa-1,4-dien-1-yl)-2,6-dimethyl-1,4-dihydropyridine-3,5-dicarboxylate (1b). The results are as follows: white solid, yield 76%; mp 168°C; IR (kBr) (cm⁻¹): 3041 (Ar-H), 2963, 2871 (C-H str of CH₃), 1755 (C=O in ester), 1630, 1640 (C=O), 840 (C-Cl); ¹H NMR (300 MHz, DMSO-d₆): 7.37-7.17 (m, 4H, Ph-Cl), 6.32 (s, 1H, -CH in TQ), 4.95 (s, 1H, CH-Ph), 4.16 (m, 4H, -(CH₂)₂), 2.53 (m, 1H, CH in TQ), 2.28 (s, 6H, 2,6-CH₃), 1.74 (s, 3H, -CH₃), 1.28 (t, 6H, -(CH₃)₂), 1.08 (d, *J* = 6.9 Hz, CH₃); ¹³C NMR (300 MHz, DMSO-d₆): 187.22, 178.54, 167.26, 153.58, 144.70, 143.83, 142.74, 142.50, 133.85, 131.30, 130.40, 128.70, 102.39, 61.80, 43.51, 21.03, 15.45, 14.27, 14.19; EI-MS: 526 (M⁺, 20%); elemental analysis (C₂₉H₃₂ClNO₆): calculated: C, 66.22; H, 6.13; N, 2.66%; found: C, 66.20; H, 6.11; N, 2.64%.

(3) Synthesis of Diethyl 4-(2-Chlorophenyl)-1-(2-isopropyl-5-methyl-3,6-dioxocyclohexa-1,4-dien-1-yl)-2,6-dimethyl-1,4-dihydropyridine-3,5-dicarboxylate (1c). The results are as follows: white solid, yield 89%; mp 184°C; IR (kBr) (cm⁻¹): 3034 (Ar-H), 2960, 2871 (C-H str of CH₃), 1741 (C=O in ester), 1665, 1623 (C=O), 840 (C-Cl); ¹H NMR (300 MHz, DMSO-d₆): 7.65-7.18 (m, 4H, Ph-Cl), 6.34 (s, 1H, -CH in TQ), 4.96 (s, 1H, CH-Ph), 4.19 (m, 4H, -(CH₂)₂), 2.54 (m, 1H, CH in TQ), 2.29 (s, 6H, 2,6-CH₃), 1.75 (s, 3H, -CH₃), 1.29 (t, 6H, -(CH₃)₂), 1.09 (d, *J* = 6.9 Hz, CH₃); ¹³C NMR (300 MHz, DMSO-d₆): 187.23, 178.55, 167.27, 153.59, 144.71, 143.84, 143.70, 142.75, 133.86, 131.40, 128.71, 127.10, 126.70, 126.41, 102.40, 61.81, 38.40, 21.04, 15.46, 14.28, 14.20; EI-MS: 526 (M⁺, 20%); elemental analysis (C₂₉H₃₂ClNO₆): calculated: C, 66.22; H, 6.13; N, 2.66%; found: C, 66.20; H, 6.11; N, 2.64%.

(4) Synthesis of Diethyl 4-(4-Hydroxyphenyl)-1-(2-isopropyl-5-methyl-3,6-dioxocyclohexa-1,4-dien-1-yl)-2,6-dimethyl-1,4-dihydropyridine-3,5-dicarboxylate (1d). The results are as follows: white solid, yield 80%; mp 204°C; IR (kBr) (cm⁻¹): 3098 (OH), 3032 (Ar-H), 2964, 2865 (C-H str of CH₃),

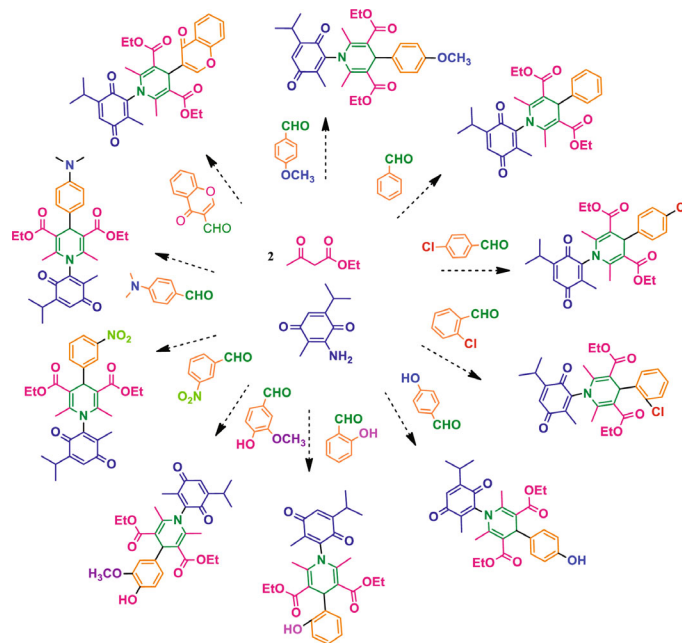
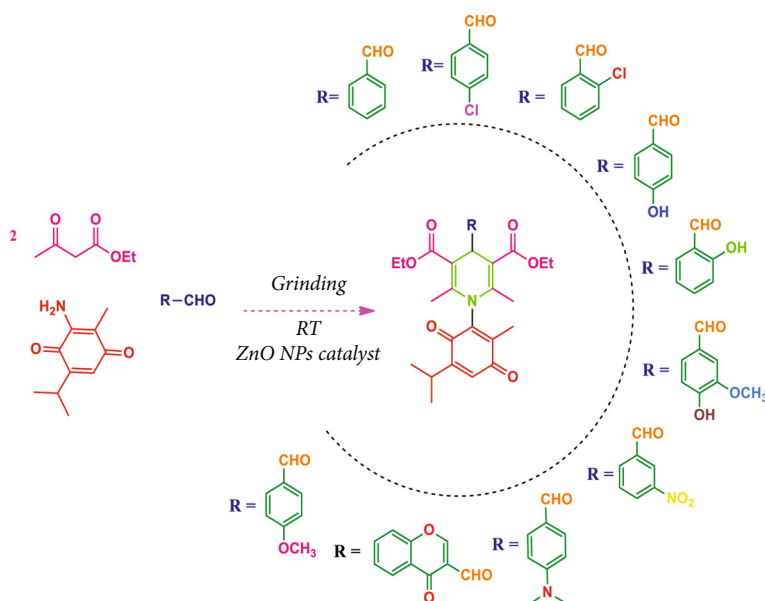


FIGURE 5: Optimization of reaction condition (1a-1j).

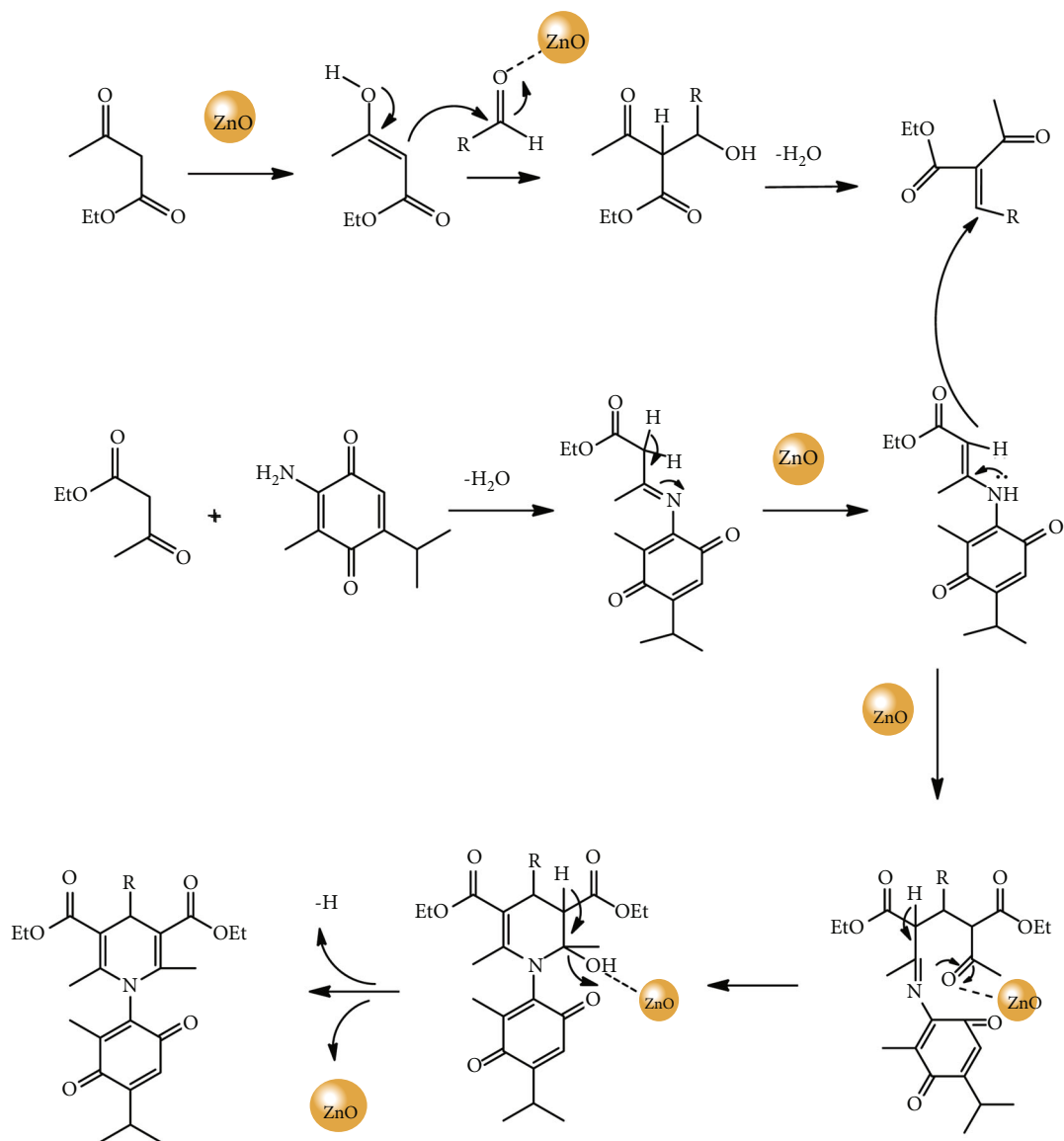


SCHEME 2: Synthesis of thymoquinone connected 1,4-dihydropyridine derivatives (1a-1j).

1764 (C=O in ester), 1652, 1638 (C=O); ^1H NMR (300 MHz, DMSO-d_6): 7.06-6.63 (m, 4H, Ph-OH), 6.35 (s, 1H, -CH in TQ), 5.37 (s, 1H, OH), 4.97 (s, 1H, CH-Ph), 4.20 (m, 4H, $-(\text{CH}_2)_2$), 2.55 (m, 1H, CH in TQ), 2.30 (s, 6H, 2,6- CH_3), 1.76 (s, 3H, $-\text{CH}_3$), 1.30 (t, 6H, $-(\text{CH}_3)_2$), 1.10 (d, $J = 6.5$ Hz, CH_3); ^{13}C NMR (300 MHz, DMSO-d_6): 187.24, 178.56, 167.28, 155.50, 153.60, 144.72, 143.85, 142.76, 137.71, 133.87, 130.40, 115.81, 102.41, 61.82, 43.52, 21.05, 15.47, 14.29, 14.21; EI-MS: 508 (M^+ , 20%); elemental analy-

sis ($\text{C}_{29}\text{H}_{33}\text{NO}_7$): calculated: C, 68.62; H, 6.55; N, 2.76%; found: C, 68.60; H, 6.53; N, 2.74%.

(5) Synthesis of Diethyl 4-(2-Hydroxyphenyl)-1-(2-isopropyl-5-methyl-3,6-dioxocyclohexa-1,4-dien-1-yl)-2,6-dimethyl-1,4-dihydropyridine-3,5-dicarboxylate (1e). The results are as follows: yellow solid, yield 90%; mp 112°C; IR (kBr) (cm^{-1}): 3089 (OH), 3069 (Ar-H), 2958, 2825 (C-H str of CH_3), 1762 (C=O in ester), 1662, 1658 (C=O); ^1H NMR



SCHEME 3: Proposed mechanism pathway for the ZnO NP catalyzed synthesis of 1,4-dihydropyridine derivatives.

TABLE 2: Cytotoxic activity of synthesized compounds (1a-1j) (μM).

Cpds	HepG2			MCF-7			Hela (Cervical)		
	GI ₅₀ (μm)	TGI (μm)	LC ₅₀ (μm)	GI ₅₀ (μm)	TGI (μm)	LC ₅₀ (μm)	GI ₅₀ (μm)	TGI (μm)	LC ₅₀ (μm)
1a	33.2	18.3	>100	—	—	>100	—	—	100
1b	22.2	13.1	36.8	26.1	25.1	>100	61.0	79.2	>100
1c	26.3	15.3	29.9	34.9	33.7	29.4	51.3	77.2	66.7
1d	01.0	0.25	14.0	0.89	09.3	25.0	08.9	16.8	55.9
1e	25.9	28.2	12.8	34.4	19.3	26.3	44.2	62.1	>100
1f	19.1	0.88	0.50	28.6	11.8	0.64	31.6	44.7	0.52
1g	1.10	1.52	0.90	24.0	57.4	1.18	47.9	41.9	0.93
1h	11.3	1.08	10.0	22.9	55.3	0.95	62.9	71.3	>100
1i	19.3	1.35	>100	55.6	66.0	9.30	59.0	59.3	65.0
1j	10.3	15.3	16.8	16.0	39.3	18.0	3.3	48.3	58.3
Doxorubicin (standard)	0.01	0.13	0.58	0.02	0.21	0.74	0.05	0.41	0.88

TABLE 3: In vitro cytotoxicity of synthesized derivatives (1a-1j) on normal cells^a.

Compounds	MRC5	HEK-293	LO2
	IC ₅₀ (μm)	IC ₅₀ (μm)	IC ₅₀ (μm)
1a	56.36	69.06	67.48
1b	77.21	62.12	70.17
1c	76.66	51.14	79.10
1d	58.25	76.14	66.24
1e	70.76	57.09	56.01
1f	89.24	88.17	80.24
1g	59.61	66.24	68.54
1h	66.32	67.01	58.22
1i	74.41	75.44	65.70
1j	71.14	52.71	70.12

^aEach compound was tested in triplicate. All error bars represent mean ± SD from three independent experiments.

(300 MHz, DMSO-d₆): 7.09-6.83 (m, 4H, Ph-OH), 6.29 (s, 1H, -CH in TQ), 5.30 (s, 1H, OH), 4.98 (s, 1H, CH-Ph), 4.21 (m, 4H, -(CH₂)₂), 2.56 (m, 1H, CH in TQ), 2.31 (s, 6H, 2,6-CH₃), 1.77 (s, 3H, -CH₃), 1.31 (t, 6H, -(CH₃)₂), 1.11 (d, *J* = 6.6 Hz, CH₃); ¹³C NMR (300 MHz, DMSO-d₆): 187.25, 178.57, 167.29, 156.10, 153.61, 144.73, 143.86, 142.77, 133.88, 130.41, 127.12, 122.61, 121.14, 102.42, 61.83, 37.52, 21.06, 15.48, 14.30, 14.22; EI-MS: 508 (M+, 20%); elemental analysis (C₂₉H₃₃NO₇): calculated: C, 68.62; H, 6.55; N, 2.76%; found: C, 68.60; H, 6.53; N, 2.74%.

(6) *Synthesis of Diethyl 4-(4-Hydroxy-3-methoxyphenyl)-1-(2-isopropyl-5-methyl-3,6-dioxocyclohexa-1,4-dien-1-yl)-2,6-dimethyl-1,4-dihydropyridine-3,5-dicarboxylate (1f)*. The results are as follows: white solid, yield 74%; mp 118°C; IR (kBr) (cm⁻¹): 3089 (OH), 3069 (Ar-H), 2961 (O-CH₃), 2918, 2865 (C-H str of CH₃), 1742 (C=O in ester), 1663, 1713 (C=O); ¹H NMR (300 MHz, DMSO-d₆): 7.09-6.83 (m, 4H, Van), 6.36 (s, 1H, -CH in TQ), 5.35 (s, 1H, OH), 4.99 (s, 1H, CH-Ph), 4.22 (m, 4H, -(CH₂)₂), 3.83 (s, 3H, -OCH₃), 2.57 (m, 1H, CH in TQ), 2.32 (s, 6H, 2,6-CH₃), 1.78 (s, 3H, -CH₃), 1.32 (t, 6H, -(CH₃)₂), 1.12 (d, *J* = 6.9 Hz, CH₃); ¹³C NMR (300 MHz, DMSO-d₆): 187.26, 178.58, 167.30, 153.62, 147.42, 145.70, 144.74, 143.87, 142.78, 135.80, 133.89, 122.71, 115.50, 114.51, 102.43, 61.84, 56.10, 21.07, 15.49, 14.31, 14.23; EI-MS: 538 (M+, 20%); elemental analysis (C₃₀H₃₅NO₈): calculated: C, 67.02; H, 6.56; N, 2.61%; found: C, 67.00; H, 6.54; N, 2.59%.

(7) *Synthesis of Diethyl 1-(2-Isopropyl-5-methyl-3,6-dioxocyclohexa-1,4-dien-1-yl)-2,6-dimethyl-4-(3-nitrophenyl)-1,4-dihydropyridine-3,5-dicarboxylate (1g)*. The results are as follows: white solid, yield 95%; mp 256°C; IR (kBr) (cm⁻¹): 3041 (Ar-H), 2960, 2875 (C-H str of CH₃), 1707 (C=O in ester), 1630, 1652 (C=O), 1540 (-NO₂); ¹H NMR (300 MHz, DMSO-d₆): 8.12-7.59 (m, 4H, PH-NO₂), 6.37 (s, 1H, -CH in TQ), 5.00 (s, 1H, CH-PH), 4.23 (m, 4H, -(CH₂)₂), 2.58 (m, 1H, CH in TQ), 2.34 (s, 6H, 2,6-CH₃), 1.79 (s, 3H,

-CH₃), 1.33 (t, 6H, -(CH₃)₂), 1.13 (d, *J* = 6.9 Hz, CH₃); ¹³C NMR (300 MHz, DMSO-d₆): 187.27, 178.59, 167.31, 153.63, 147.90, 145.21, 144.75, 143.88, 142.79, 134.20, 133.90, 121.80, 121.12, 120.91, 102.44, 61.85, 42.52, 21.08, 15.50, 14.32, 14.24; EI-MS: 537 (M+, 20%); elemental analysis (C₂₉H₃₂N₂O₈): calculated: C, 64.64; H, 7.16; N, 5.22%; found: C, 64.62; H, 7.14; N, 5.00%.

(8) *Synthesis of Diethyl 4-(4-(Dimethylamino)phenyl)-1-(2-isopropyl-5-methyl-3,6-dioxo cyclohexa-1,4-dien-1-yl)-2,6-dimethyl-1,4-dihydropyridine-3,5-dicarboxylate (1h)*. The results are as follows: yellow yield 79%; mp 184°C; IR (kBr) (cm⁻¹): 3072 (Ar-H), 2968, 2875, 2953, 2966 (C-H str of CH₃), 1761 (C=O in ester), 1665, 1623 (C=O); ¹H NMR (300 MHz, DMSO-d₆): 6.95-6.64 (m, 4H, Ph), 6.38 (s, 1H, -CH in TQ), 5.01 (s, 1H, CH-Ph), 4.24 (m, 4H, -(CH₂)₂), 3.06 (s, 6H, -(CH₃)₂), 2.59 (m, 1H, CH in TQ), 2.35 (s, 6H, 2,6-CH₃), 1.80 (s, 3H, -CH₃), 1.34 (t, 6H, -(CH₃)₂), 1.14 (d, *J* = 6.9 Hz, CH₃); ¹³C NMR (300 MHz, DMSO-d₆): 187.29, 178.61, 167.33, 153.65, 148.10, 144.77, 143.90, 142.81, 133.99, 133.92, 128.10, 112.01, 102.46, 61.87, 41.73, 21.10, 15.52, 14.34, 14.26; EI-MS: 535 (M+, 20%); elemental analysis (C₃₁H₃₈N₂O₆): calculated: C, 69.64; H, 7.16; N, 5.24%; found: C, 69.62; H, 7.14; N, 5.22%.

(9) *Synthesis of Diethyl 1-(2-Isopropyl-5-methyl-3,6-dioxocyclohexa-1,4-dien-1-yl)-2,6-dimethyl-4-(4-oxo-4H-chromen-3-yl)-1,4-dihydropyridine-3,5-dicarboxylate (1i)*. The results are as follows: white solid, yield 70%; mp 128°C; IR (kBr) (cm⁻¹): 3065 (Ar-H), 2948, 2871 (C-H str of CH₃), 1750 (C=O in ester), 1713, 1625 (C=O); ¹H NMR (300 MHz, DMSO-d₆): 8.08-6.90 (m, 5H, Chromene-3-carbaldehyde), 6.39 (s, 1H, -CH in TQ), 5.02 (s, 1H, CH-Ph), 4.25 (m, 4H, -(CH₂)₂), 3.00 (m, 1H, CH in TQ), 2.36 (s, 6H, 2,6-CH₃), 1.81 (s, 3H, -CH₃), 1.35 (t, 6H, -(CH₃)₂), 1.15 (d, *J* = 6.8 Hz, CH₃); ¹³C NMR (300 MHz, DMSO-d₆): 187.28, 183.01, 178.60, 167.32, 157.20, 153.64, 151.60, 144.76, 143.89, 142.80, 135.20, 133.91, 125.80, 123.91, 123.42, 116.10, 115.31, 102.45, 61.86, 43.71, 21.09, 15.51, 14.33, 14.25; EI-MS: 560 (M+, 20%); elemental analysis (C₃₂H₃₃NO₈): calculated: C, 68.68; H, 5.94; N, 2.50%; found: C, 68.66; H, 5.92; N, 2.48%.

(10) *Synthesis of Diethyl 1-(2-Isopropyl-5-methyl-3,6-dioxocyclohexa-1,4-dien-1-yl)-4-(4-methoxyphenyl)-2,6-dimethyl-1,4-dihydropyridine-3,5-dicarboxylate (1j)*. The results are as follows: white solid, yield 89%; mp 152°C; IR (kBr) (cm⁻¹): 3070 (Ar-H), 2961 (O-CH₃), 2960, 2851 (C-H str of CH₃), 1747 (C=O in ester), 1743, 1630 (C=O); ¹H NMR (300 MHz, DMSO-d₆): 7.12-6.87 (m, 4H, Ph-OCH₃), 6.40 (s, 1H, -CH in TQ), 5.03 (s, 1H, CH-Ph), 4.25 (m, 4H, -(CH₂)₂), 3.83 (s, 3H, OCH₃), 3.01 (m, 1H, CH in TQ), 2.37 (s, 6H, 2,6-CH₃), 1.82 (s, 3H, -CH₃), 1.36 (t, 6H, -(CH₃)₂), 1.18 (d, *J* = 6.4 Hz, CH₃); ¹³C NMR (300 MHz, DMSO-d₆): 187.30, 178.62, 167.34, 157.60, 153.66, 144.78, 143.91, 142.82, 136.70, 133.93, 130.00, 114.20, 102.46, 61.87, 55.80, 43.59, 21.11, 15.53, 14.35, 14.27; EI-MS: 522 (M+, 20%); elemental analysis (C₃₀H₃₅NO₇): calculated: C, 69.08; H, 6.76; N, 2.69%; found: C, 69.06; H, 6.74; N, 2.67%.

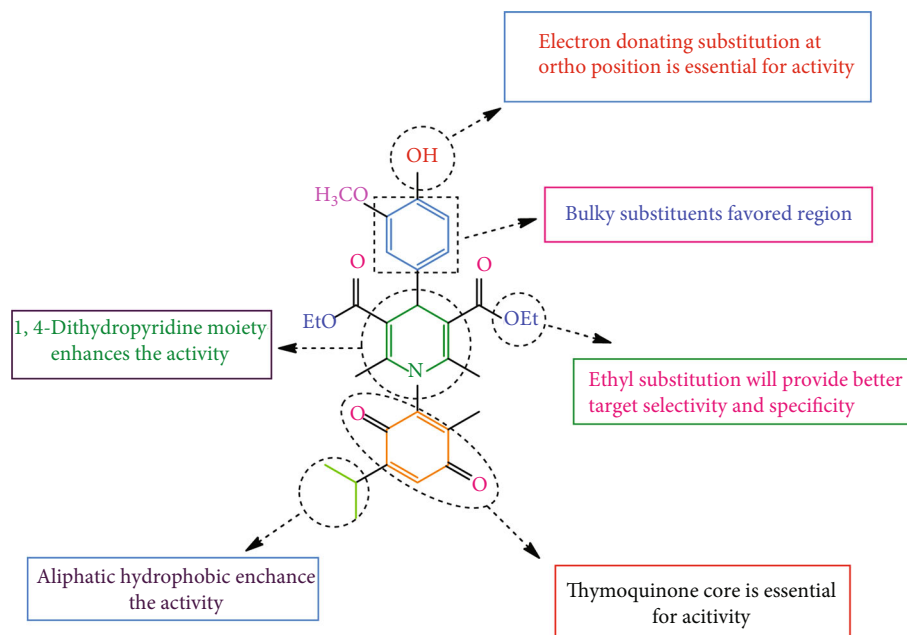


FIGURE 6: SAR of highly active compound.

2.1.4. Cytotoxic Activity. The cytotoxicity test was carried out according to a protocol established by the National Cancer Institute in the United States [46].

3. Results and Discussion

3.1. Characterization of Silver Nanoparticles

3.1.1. Scanning Electron Microscopy (SEM). SEM image has showed individual zinc particles as well as a number of aggregates. The SEM image revealed a spherical-shaped nanoparticle with a diameter of 12-27 nm. Figure 2 shows the formation of aggregated molecules in the 12 m range.

3.1.2. Transmission Electron Microscopy (TEM). To learn more about the size and morphology of the ZnO NPs, a TEM study was performed. TEM images of ZnO NPs at different magnifications are shown in Figures 3(a) and 3(b). The average particle size of ZnO NPs can be seen in the TEM images in the range of 16–27 nm.

3.1.3. Catalyst Recovery Studies. Figure 4 demonstrates the recovery of the catalyst with a small loss of catalytic activity after at least 12-15 run times. By optimising the reaction conditions, the application of the catalyst was examined. Table 1 shows the yield of a number of aldehydes used in the condensation reaction with the ZnO-NP (1 mole percent) catalyst at room temperature in a solvent-free setting.

3.2. Chemistry. All the newly synthesized thymoquinone derivatives were characterized by FT-IR, which showed various functional groups. The $^1\text{H-NMR}$ spectra of compounds (**1a-1j**) indicate frequency observed at 7.16-7.07 and 6.79-5.54, corresponding to the NH-CH and CH-Ph protons. The $^{13}\text{C-NMR}$ spectra exhibit the peak at 144.42-118.76 and 40.60-40.53, corresponding to the NH-CH and CH-Ph

carbon, respectively. Optimization of reaction condition (**1a-1j**) is shown in Figure 5. The synthetic pathway of thymoquinone derivatives is shown in Scheme 2. The possible mechanism for the coupling of aldehydes, dimedone, and amines in the presence of ZnO NPs as an effective catalyst is shown in Scheme 3. To the best of our knowledge, ZnO NPs catalyze the reaction by electrophilic activation of the carbonyl groups of aldehydes and ethyl acetoacetate; this makes them susceptible to nucleophilic attack.

3.2.1. Cytotoxic Activity. The cytotoxic activity of the newly prepared compounds **1a-1j** is tested using the US NCI protocol, which was previously recorded [46]. The values for growth inhibition at 50% (GI_{50}), tumour growth inhibition (TGI), and lethal concentration (LC_{50}) were calculated. The compounds **1f** have a significant activity against HepG2, LC_{50} -0.50 μM , MCF-7, LC_{50} -0.64 μM , HeLa, and LC_{50} -0.52 μM . Doxorubicin was used as a standard drug. Using the MTT assay, the compounds were tested for cytotoxicity in human embryonic kidney cells (HEK-293), lung cells (MRC-5), and liver cells (LO2). Since most of the compound's IC_{50} values are greater than 100, the assay results indicated that these compounds had no significant effect on normal kidney cell growth. As a result, compound **1f** can be used as a lead compound for the production of more potent agents for cancer cell lines HepG2 (liver), MCF-7 (breast), and HeLa (cervical). Table 2 shows the effects of cytotoxic screening of compounds (**1a-1j**), and Table 3 shows the cytotoxicity screening of normal cell lines.

3.3. Structure-Activity Relationship. The aim of a structure-activity relationship study (SAR) was to discover a correlation between a dynamic molecule's chemical structure and its cytotoxic activity. The chemical group/atom that plays a critical role in modulating the cytotoxic activity of

compounds within a particular system can be identified using SAR analysis. Using the 1,4-dihydropyridine derivative's cytotoxic behaviour findings, the data of the selected 1,4-dihydropyridine derivatives (**1a-1j**) showed that compound **1f** is the most effective (HepG2, LC₅₀-0.50 μ M, MCF-7, LC₅₀-0.64 μ M, HeLa, and LC₅₀-0.52 μ M) control doxorubicin. The fundamental SAR could be assessed and is shown in Figure 6.

It was discovered that the compound **1f** has a high cytotoxic activity against cancer cell lines due to the presence of a 1,4-dihydropyridine ring fused to a vanillin. The presence of a OH moiety on a phenyl ring attached to a 1,4-dihydropyridine skeleton caused this. The remaining compounds have only moderate cytotoxic activity against all of the cancer cell lines.

4. Conclusion

We have developed an environmentally friendly new method for the high yield synthesis of 3-amino thymoquinone connected 1,4-dihydropyridine derivatives (**1a-1j**) using ZnO as nanoparticle catalyst. Three cancer cell lines and normal cell lines were used to assess the cytotoxic activity of the 1,4-dihydropyridine derivatives. MTT assay was performed using doxorubicin as the standard drug on human embryonic kidney cell (HEK293), liver cell (LO2), and lung cell (MRC5). Compound **1f** (HepG2, LC₅₀-0.50 μ M, MCF-7, LC₅₀-0.64 μ M, HeLa, and LC₅₀-0.52 μ M) was found to be highly active when compared with other compounds. Therefore, compound **1f** could provide as a high momentous molecule for further development of an anticancer drug.

Data Availability

Supplementary information is associated with this submission.

Conflicts of Interest

The authors declare no conflict of interest.

Acknowledgments

The authors extend their appreciation to the Researchers supporting project number RSP-2021/316, King Saud University, Riyadh, Saudi Arabia.

Supplementary Materials

The supplementary material used to support the findings of this study is included within the supplementary information files. (The supplementary file contains ¹H-NMR and ¹³C-NMR spectra). (*Supplementary Materials*)

References

- [1] C. B. Blackadar, "Historical review of the causes of cancer," *World Journal of Clinical Oncology*, vol. 7, no. 1, pp. 54–86, 2016.
- [2] P. S. Roy and B. J. Saikia, "Cancer and cure: a critical analysis," *Indian Journal of Cancer*, vol. 53, no. 3, pp. 441–442, 2016.
- [3] Report, W, *WHO Cancer Report*, WHO, 2019.
- [4] S. K. Carter, M. Bakowski, and K. Hellman, *Chemotherapy of Cancer*, John Wiley and Sons Inc, USA, 3rd edition, 1987.
- [5] S. Srivastava, E. J. Koay, A. D. Borowsky et al., "Cancer overdiagnosis: a biological challenge and clinical dilemma," *Nature Reviews. Cancer*, vol. 19, no. 6, pp. 349–358, 2019.
- [6] C. C. Woo, A. P. Kumar, G. Sethi, and K. H. B. Tan, "Thymoquinone: potential cure for inflammatory disorders and cancer," *Biochemical Pharmacology*, vol. 83, no. 4, pp. 443–451, 2012.
- [7] H. U. Gali-Muhtasib, W. G. Abou Kheir, L. A. Kheir, N. Darwiche, and P. A. Crooks, "Molecular pathway for thymoquinone-induced cell-cycle arrest and apoptosis in neoplastic keratinocytes," *Anti-Cancer Drugs*, vol. 15, no. 4, pp. 389–399, 2004.
- [8] M. El-Dakhkhny, "Studies on the chemical constitution of Egyptian *Thymus sativa* L. seeds. II¹) The essential oil," *Planta Medica*, vol. 11, no. 4, pp. 465–470, 1963.
- [9] O. A. Badary, O. A. Al-Shabanah, M. N. Nagi, A. C. Al-Rikabi, and M. M. Elmazar, "Inhibition of benzo(a)pyrene-induced forestomach carcinogenesis in mice by thymoquinone," *European Journal of Cancer Prevention*, vol. 8, no. 5, pp. 435–440, 1999.
- [10] S. Attoub, O. Sperandio, H. Raza et al., "Thymoquinone as an anticancer agent: evidence from inhibition of cancer cells viability and invasion in vitro and tumor growth in vivo," *Fundamental & Clinical Pharmacology*, vol. 27, no. 5, pp. 557–569, 2013.
- [11] R. Schneider-Stock, I. H. Fakhoury, A. M. Zaki, C. O. El-Baba, and H. U. Gali Muhtasib, "Thymoquinone: fifty years of success in the battle against cancer models," *Drug Discovery Today*, vol. 19, no. 1, pp. 18–30, 2014.
- [12] H. Gali-Muhtasib, M. Diab-Assaf, C. Boltze et al., "Thymoquinone extracted from black seed triggers apoptotic cell death in human colorectal cancer cells via a p53-dependent mechanism," *International Journal of Oncology*, vol. 25, no. 4, pp. 857–866, 2004.
- [13] M. Roepke, A. Diestel, K. Bajbouj et al., "Lack of p53 augments thymoquinone-induced apoptosis and caspase activation in human osteosarcoma cells," *Cancer Biology & Therapy*, vol. 6, no. 2, pp. 160–169, 2007.
- [14] P. S. Koka, D. Mondal, M. Schultz, A. B. Abdel-Mageed, and K. C. Agrawal, "Studies on molecular mechanisms of growth inhibitory effects of thymoquinone against prostate cancer cells: role of reactive oxygen species," *Experimental Biology and Medicine*, vol. 235, no. 6, pp. 751–760, 2010.
- [15] N. El-Najjar, M. Chatila, H. Moukadem et al., "Reactive oxygen species mediate thymoquinone-induced apoptosis and activate ERK and JNK signaling," *Apoptosis*, vol. 15, no. 2, pp. 183–195, 2010.
- [16] E. M. Dergarabetian, K. I. Ghattass, S. B. El-Sitt et al., "Thymoquinone induces apoptosis in malignant T-cells via generation of ROS," *Frontiers in Bioscience*, vol. 5, no. 2, pp. 706–719, 2013.
- [17] M. C. Chen, N. H. Lee, H. H. Hsu et al., "Inhibition of NF- κ B and metastasis in irinotecan (CPT-11)-resistant LoVo colon cancer cells by thymoquinone via JNK and p38," *Environmental Toxicology*, vol. 32, no. 2, pp. 669–678, 2017.

- [18] B. Iskender, K. Izgi, and H. Canatan, "Novel anti-cancer agent myrtoquinnone-A and thymoquinone abrogate epithelial-mesenchymal transition in cancer cells mainly through the inhibition of PI3K/AKT signalling axis," *Molecular and Cellular Biochemistry*, vol. 416, no. 1-2, pp. 71-84, 2016.
- [19] O. A. Badary, O. A. Al-Shabanah, M. N. Nagi, A. M. Al-Bekairi, and M. M. A. Elmazar, "Acute and subchronic toxicity of thymoquinone in mice," *Drug Development Research*, vol. 44, no. 2-3, pp. 56-61, 1998.
- [20] A. Al-Ali, A. A. Alkhawajah, M. A. Randhawa, and N. A. Shaikh, "Oral and intraperitoneal LD50 of thymoquinone, an active principle of *Nigella sativa*, in mice and rats," *Journal of Ayub Medical College, Abbottabad*, vol. 20, pp. 25-27, 2008.
- [21] M. AbuKhader, "Thymoquinone in the clinical treatment of cancer: fact or fiction?," *Pharmacognosy Reviews*, vol. 7, no. 14, pp. 117-120, 2013.
- [22] M. Tan, A. Norwood, M. May, M. Tucci, and H. Benghuzzi, "Effects of (-)-epigallocatechin gallate and thymoquinone on proliferation of a PANC-1 cell line in culture," *Biomedical Sciences Instrumentation*, vol. 42, pp. 363-371, 2006.
- [23] S. H. Jafri, J. Glass, R. Shi, S. Zhang, M. Prince, and H. Kleiner-Hancock, "Thymoquinone and cisplatin as a therapeutic combination in lung cancer: In vitro and in vivo," *Journal of Experimental & Clinical Cancer Research*, vol. 29, no. 1, pp. 87-97, 2010.
- [24] J. P. Wan and Y. Pan, "Recent advance in the pharmacology of dihydropyrimidinone," *Mini-Reviews in Medicinal Chemistry*, vol. 12, no. 4, pp. 337-349, 2012.
- [25] J. T. David, "The 1,4-dihydropyridine nucleus: a pharmacophoric template part 1. Actions at ion channels," *Mini Reviews in Medicinal Chemistry*, vol. 3, no. 3, pp. 215-223, 2003.
- [26] L. Yet, "1,4-Dihydropyridines," *1,4-Dihydropyridines. In Privileged Structures in Drug Discovery: Medicinal Chemistry and Synthesis*, pp. 59-82, Wiley, 2018.
- [27] A. K. Samrat and B. A. Pratibha, "1, 4-Dihydropyridines: a class of pharmacologically important molecules," *Mini-Reviews in Medicinal Chemistry*, vol. 14, no. 3, pp. 282-290, 2014.
- [28] E. Carosati, P. Ioan, M. Micucci et al., "1,4-Dihydropyridine scaffold in medicinal chemistry, the story so far and perspectives (part 2): action in other targets and antitargets," *Current Medicinal Chemistry*, vol. 19, no. 25, pp. 4306-4323, 2012.
- [29] M. Abhinav Prasoon, B. Ankit, and R. Awani Kumar, "1,4-Dihydropyridine: a dependable heterocyclic ring with the promising and the most anticipable therapeutic effects," *Mini Reviews in Medicinal Chemistry*, vol. 19, pp. 1219-1254, 2019.
- [30] G. Li and J. C. Antilla, "Highly enantioselective hydrogenation of enamides catalyzed by chiral phosphoric acids," *Organic Letters*, vol. 11, no. 5, pp. 1075-1078, 2009.
- [31] A. Hantzsch, "Ueber die synthese pyridinartiger verbindungen aus acetessigäther und aldehydammoniak," *Justus Liebigs Annalen der Chemie*, vol. 215, no. 1, pp. 1-82, 1882.
- [32] U. Eisner and J. Kuthan, "Chemistry of dihydropyridines," *Chemical Reviews*, vol. 72, no. 1, pp. 1-42, 1972.
- [33] A. Dömling and I. Ugi, "Multicomponent reactions with isocyanides," *Angewandte Chemie International Edition*, vol. 39, no. 18, pp. 3168-3210, 2000.
- [34] A. Dömling, "Recent developments in isocyanide based multicomponent reactions in applied chemistry," *Chemical Reviews*, vol. 106, no. 1, pp. 17-89, 2006.
- [35] S. G. Cedric, V. R. Felipe, R. R. Kamilla, and E. K. Arthur, "Multicomponent reactions for the synthesis of bioactive compounds: a review," *Current Organic Synthesis*, vol. 16, no. 6, pp. 855-899, 2019.
- [36] E. M. de Marigorta, J. M. D. L. Santos, A. M. Ochoa de Retana, J. Vicario, and F. Palacios, "Multicomponent reactions (MCRs): a useful access to the synthesis of benzo-fused γ -lactams," *Beilstein Journal of Organic Chemistry*, vol. 15, pp. 1065-1085, 2019.
- [37] O. Ghashghaei, F. Seghetti, and R. Lavilla, "Selectivity in multiple multicomponent reactions: types and synthetic applications," *Beilstein Journal of Organic Chemistry*, vol. 15, pp. 521-534, 2019.
- [38] C. Lambruschini, A. Basso, and L. Banfi, "Integrating biocatalysis and multicomponent reactions," *Drug Discovery Today: Technologies*, vol. 29, pp. 3-9, 2018.
- [39] M. Driowya, A. Saber, H. Marzag, L. Demange, K. Bougrin, and R. Benhida, "Microwave-assisted syntheses of bioactive seven-membered, Macro-Sized Heterocycles and Their Fused Derivatives," *Molecules*, vol. 21, no. 8, p. 1032, 2016.
- [40] E. Ruijter and R. V. Orru, "Multicomponent reactions - opportunities for the pharmaceutical industry," *Drug Discovery Today: Technologies*, vol. 10, no. 1, pp. e15-e20, 2013.
- [41] B. B. Touré and D. G. Hall, "Natural product synthesis using multicomponent reaction strategies," *Chemical Reviews*, vol. 109, no. 9, pp. 4439-4486, 2009.
- [42] M. A. Zolfigol, E. Kolvari, A. Abdoli, and M. Shiri, "Synthesis of new tripodal Hantzsch 1,4-dihydropyridines under solvent-free condition and their conversion to the corresponding tripodal pyridines," *Molecular Diversity*, vol. 14, no. 4, pp. 809-813, 2010.
- [43] G. Mehta and V. Singh, "Hybrid systems through natural product leads: an approach towards new molecular entities," *Chemical Society Reviews*, vol. 31, no. 6, pp. 324-334, 2002.
- [44] C. Reiter, A. Hermann, A. Çapcı, T. Efferth, and S. B. Tsogoeva, "New artesunic acid homodimers: Potent reversal agents of multidrug resistance in leukemia cells," *Bioorganic & Medicinal Chemistry*, vol. 20, no. 18, pp. 5637-5641, 2012.
- [45] T. Fröhlich, A. Çapcı Karagöz, C. Reiter, and S. B. Tsogoeva, "Artemisinin-Derived Dimers: Potent Antimalarial and Anticancer Agents," *Journal of Medicinal Chemistry*, vol. 59, no. 16, pp. 7360-7388, 2016.
- [46] P. Skehan, R. Storeng, D. Scudiero et al., "New colorimetric cytotoxicity assay for anticancer-drug screening," *Journal of the National Cancer Institute*, vol. 82, no. 13, pp. 1107-1112, 1990.